



A 1D thermoelastic response of skin tissue due to ramp-type heating via a fractional-order Lord–Shulman model

Ashraf M. Zenkour ^{a,b,*}, Tariq Saeed ^{b,c}, Ahlam A. Al-Raezah ^{a,d}

^aDepartment of Mathematics, Faculty of Science, King Abdulaziz University, Jeddah 21589, Saudi Arabia

^bDepartment of Mathematics, Faculty of Science, Kafrelsheikh University, Kafrelsheikh 33516, Egypt

^cFinancial Mathematics and Actuarial Science (FMAS)-Research Group, Department of Mathematics, Faculty of Science, King Abdulaziz University, Jeddah 21589, Saudi Arabia

^dDepartment of Mathematics, Faculty of Science, King Khalid University, Abha 9004, Saudi Arabia

Abstract

This paper presents a new mathematical perfect of fractional order to deal with the response of skin tissue subjected to ramp-type heating based on the refined Lord–Shulman generalized thermoelasticity model. Three different models; the classical, the simple Lord–Shulman as well as the refined Lord–Shulman will be discussed. The governing equivalences of the present three models are attained. The general solution for the initial and boundary condition problem is found by employing the Laplace transform approach and its inverse. Numerical results are represented in figures with a comparison to the different theories with different values of fractional order to discuss the impact of the fractional order on temperature, displacement, and dilatation distributions. The effect of ramp-type heat is studied numerically and graphically on distributions of temperature, displacement, and dilatation according to different theories.

Keywords: Refined Lord–Shulman theory; fractional calculus; Laplace transforms; bio-heat response; skin tissue; ramp-type.

1. Introduction

In 1678, the scientist Robert Hooke defined the elastic body and the word elasticity, where he put the first law linking the force acting on an elastic body and the amount of elongation (strain) that happened in the body. The mathematician Cauchy established the theory of elasticity in the seventeenth century. This scientific field offered mathematicians a variety of difficulties throughout its historical growth, some of which helped to build or were the sole source of the creation of sophisticated mathematical theories like the variational calculus and the finite element method [1].

Over the past 50 years, the use of biothermal models has grown significantly. During medical and clinical procedures, heat carry must be applied to the skin. Numerous bioheat applications have made use of the straightforward dual-phase-lage (DPL) model. A thermal loading that is called ramp-type heat can be employed to replicate the influences on skin tissue of being exposed to a gradual rise or fall in temperature over time. There are numerous practical applications for ramp-type heating, including medical procedures. Cryotherapy, for instance, involves exposing the concerned area of the organization to extremely low temperatures for a brief period during cryotherapy sessions [2].

Duhamel and Neumann set the foundation for the thermoelastic hypothesis in the first part of the nineteenth century. They provided equations that included the known function for heat in the equation of motion independent of

* Corresponding author.

E-mail address: zenkout@kau.edu.sa

mechanical forces. Biot developed the linked dynamical theory of thermoelasticity [3]. This theory is in agreement with practical investigations since it comprises the elasticity equations related to heat conductivity. The elastic body becomes tensed if there is a temperature change. A hyperbolic partial differential equation for the equation of motion and a parabolic partial differential equation for the equation of heat conduction make up the so-called conundrum in Biot's theory [3]. By Lord and Shulman (L-S) [4], one of the generalized thermoelasticity theories is produced. Green and Lindsay (G-L) [5] produce a further theory with two thermal relaxation time parameters. Then some articles appeared as Chandrasekharaiah [6] and Hetnarski and Ignaczak [7] to discuss such generalized theories. Also, the generalized thermoelasticity theory is elaborately realized in the book by Ignaczak and Martin [8]. Sherief [9] discussed the basic solution of the thermoelastic issue for a short time. The uniqueness and reciprocity theories for thermo-viscoelasticity with two relaxations were first presented by Ezzat and El-Karamany [10]. The underlying reason of electro-micro stretch viscoelastic solids and the transmission of plane waves were both investigated by Sharma et al. [11]. Othman and Abd-Elaziz [12], Sharma and Kumar [13], and Lata et al. [14] explored the plane waves, respectively in thermo-viscoelastic and elastic media. Hobiny and Abbas [15] looked at analytical answers for the rise in skin tissue temperature brought on by moving heating sources. For an infinite annular cylinder with temperature-dependent physical properties, Zenkour and Abbas [16] investigate the topic of generalized thermoelasticity with a single relaxation period.

Green and Naghdi (G-N) [17–19] presented a distinct generalized thermoelasticity theory, which at the time was regarded as a different way to formulate heat transmission, and they very consistently incorporated thermal pulse transmission into their idea. Three models are included in this hypothesis, and they are afterward known as thermoelastic theories of types G-N I, G-N II, and G-N III. This theory's central idea is that an entropy balancing law is utilized in place of the conventional entropy production inequality, and the temperature gradient and thermal displacement gradient are supposed to be the constitutive quantities [7]. The G-N I type is plagued by the paradox of infinite heat propagation velocity because it is closely related to the classical thermoelasticity theory, whereas the first two models are specific examples of the G-N III model. The G-N II model does not exhibit thermal energy dissipation since there is no alteration in internal energy. As a result, it suggests that the internal rate of generation of entropy is virtually zero, which is inconsistent with the G-N III model's general case. Numerous studies have examined different theoretical and practical elements of thermoelasticity within the situation of G-N II or III theories. Chandrasekharaiah [20] utilized the energy approach, uniqueness theorems were proven.

Kumar et al. [21] investigated PL effects in skin tissue midst temporary heating. Sharma et al. [22] studied the G-N II and III theories to investigate how viscosity affected wave propagation in anisotropic thermoelastic materials. Chirita and Ciarletta [23] developed the reciprocal and variational concepts in linear thermoelasticity without energy dissipation. Ghazanfarian et al. [24] created a theory of micropolar thermoelasticity without energy loss. Phase-lagging heat transfer has received a lot of interest recently due to its promising performance in testing over a variety of lengths and time scales. By carefully selecting the parameters, Othman and Abbas [25] were able to resolve the thermal shock problem for hollow cylinders in generalized thermoelasticity, which was based on the G-N II and III theories. In the theory of thermoelasticity, a 2D problem for a sphere was resolved by Sherief and Raslan [26]. Zenkour et al. [27] evolved a new G-L theory of thermoelasticity that was created as a result of changes made to thermodynamics theories and their applications in biomathematics. The conveyances of field amounts are researched by utilizing the refined G-L bio-heat move model.

Fractional analytics has recently been used effectively in numerous fields to change many occurring models of physical activities, including chemistry, biology, modeling and identification, hardware, wave proliferation, and viscoelasticity [28–30]. Abbas [31] pondered the issue of fractional-order thermoelastic interaction in a medium subjected to a traveling heat source and magnetic field. Fractional-order models frequently perform incredibly well, especially for dielectrics and viscoelastic materials over wide time and recurrence ranges [32, 33]. Free convection effects on a viscoelastic boundary layer flow with one relaxation time over a porous media were developed by Ezzat and Abd-Elal [34]. In addition to introducing a fractional formula for heat conduction, Sherief et al. [35, 36] also established an individuality theorem, deduced a reciprocity relation, and introduced a variational principle. Hendy et al. [37] presented a two-temperature fractional G-N III theory to discuss the magneto-thermo-viscoelastic response of a medium under a moving heat source. A theory of heat conduction on a deformable medium that depends on the conductive temperature and the dynamic temperature was devised by Chen and Gurtin [38]. Ezzat and Awad [39] devised the theory of micropolar-generalized two-temperature thermoelasticity, and the formulation is then applied to a thermal shock half-space issue. The current work aims to create a 1D refined Lord–Shulman (L-S) theory restraint of skin tissue with fractional-order subject to ramp-type heat.

Fractional calculus is used to extend standard differentiation and integration to non-integer order. Integration and differentiation are included in the definition of a fractional derivative. Studies and findings derived from solutions to fractional differential equations are more widespread and equally stable as those derived from their counterparts of integer order. For scholars in a variety of disciplines, including physics, engineering, biology, etc., fractional calculus

has been a rich subject. It is crucial to the study of our lives [40, 41].

Fractional differential operators can be defined in a variety of ways, including Grunwald–Letnikov, Riemann–Liouville, Caputo, and Hadamard. The two techniques most frequently employed in applications are Riemann–Liouville and Caputo's. The first use of fractional derivatives was by Abel to solve an integral equation using fractional calculus. Caputo defined the fractional derivatives of order $0 < \alpha < \frac{1}{3}$ for the continuous function. When using fractional derivatives to explain viscoelastic materials, Caputo and Mainardi found a connection between them and the theory of linear viscoelasticity [42].

1.1. Caputo–type fractional derivative

Let $\alpha > 0 \in \mathcal{R}, k = [\alpha]$, and f be a continuous function over (a, b) . Then, the Caputo fractional derivative is expressed as [43]

$${}_0 D_t^\alpha f(t) = \frac{1}{\Gamma(n-\alpha)} \int_0^t \frac{f^{(n)}(\tau)}{(t-\tau)^{\alpha+1-n}} d\tau, \quad n-1 < \alpha < n. \quad (1)$$

1.2. Laplace transform of Caputo–type fractional derivative

The Caputo-derivative Laplace transform is stated as [44]

$$\mathcal{L}\{D_t^\alpha f(t)\} = s^\alpha F(s) - \sum_{k=1}^n s^{\alpha-k} [D_t^k f(0)], \quad n-1 < \alpha < n. \quad (2)$$

2. Governing equations

According to [44], Fourier's law links the temperature gradient $\nabla\theta$ and the heat flux vector \vec{q} as

$$\vec{q}(\vec{x}, t) = -k_t \nabla\theta(\vec{x}, t). \quad (3)$$

Such that, $\theta = T - T_b$ is the essential temperature of the tissue. The energy equation is given by [45]

$$\rho_t c_t \frac{\partial \theta}{\partial t} + \gamma_t T_0 \frac{\partial}{\partial t} (\text{div } \vec{u}) = -\nabla \cdot \vec{q} + Q, \quad (4)$$

where \vec{u} is displacement vector and $\text{div } \vec{u} = e = e_{kk}$ is volumetric strain, e_{ij} is the strain tensor, and γ_t is the thermal constant factor whose relation with the thermal expansion coefficient α_t is $\gamma_t = (2\mu_t + 3\lambda_t)\alpha_t$. The heat source of Q for biological tissue can be written as

$$Q = w_b \rho_b c_b (T_b - T) + Q_L + Q_m, \quad (5)$$

where w_b is the rate of blood perfusion.

The CTE theory, which uses Fourier's law to generate the heat conduction equation, is one of the core theories of linked thermoelasticity. The Fourier law was changed by the Cattaneo–Vernotte model of thermal conductivity. This model, which is described by Sobhy and Zenkour [46], includes a relaxation time, a heat flow, and its temporal derivatives

$$\left(1 + \sum_{n=1}^N \frac{\tau^n}{n!} \frac{\partial^n}{\partial t^n}\right) \vec{q} = -k_t \nabla\theta. \quad (6)$$

The simple Lord–Shulman theory, simple (L–S) is assigned by [46]

$$k_t \nabla^2 \theta = \left(1 + \tau \frac{\partial}{\partial t}\right) \left[\frac{\partial}{\partial t} (\rho_t c_t \theta + \gamma_t T_b e) + w_b \rho_b c_b \theta - Q_m - Q_r\right], \quad (7)$$

and the refined L–S generalized thermoelasticity theory is granted by [46]

$$k_t \nabla^2 \theta = \left(1 + \sum_{n=1}^N \frac{\tau^n}{n!} \frac{\partial^n}{\partial t^n}\right) \left[\frac{\partial}{\partial t} (\rho_t c_t \theta + \gamma_t T_b e) + w_b \rho_b c_b \theta - Q_m - Q_r\right], N \geq 1, \quad (8)$$

Now, by taking the time-fractional heat conduction on equations (6)–(8), we obtain

$$\left(1 + \sum_{n=1}^N \frac{\tau^{n+\nu}}{(n+\nu)!} \frac{\partial^{n+\nu}}{\partial t^{n+\nu}}\right) \vec{q} = -k_t \nabla \theta, \quad (9)$$

where $0 < \nu < 1$.

The CTE theory is given by

$$k_t \nabla^2 \theta = \frac{\partial^{1+\nu}}{\partial t^{1+\nu}} (\rho_t c_t \theta + \gamma_t T_b e) + w_b \rho_b c_b \theta - Q_L - Q_m. \quad (10)$$

The simple L–S theory is given in the form

$$k_t \nabla^2 \theta = \left(1 + \frac{\tau^{1+\nu}}{(1+\nu)!} \frac{\partial^{1+\nu}}{\partial t^{1+\nu}}\right) \left[\frac{\partial}{\partial t} (\rho_t c_t \theta + \gamma_t T_b e) + w_b \rho_b c_b \theta - Q_m - Q_L\right], \quad (11)$$

and the refined L–S generalized thermoelasticity theory

$$k_t \nabla^2 \theta = \left(1 + \sum_{n=1}^N \frac{\tau^{n+\nu}}{(n+\nu)!} \frac{\partial^{n+\nu}}{\partial t^{n+\nu}}\right) \left[\frac{\partial}{\partial t} (\rho_t c_t \theta + \gamma_t T_b e) + w_b \rho_b c_b \theta - Q_m - Q_L\right], \quad N \geq 1, \quad (12)$$

It is to be noted that the CTE is obtained by sitting $\tau = 0$ on (12) and the simple L–S by sitting $N = 1$ in equation (12).

For the sitting one-dimensional problem, the constitutive relations reduced to

$$\sigma = (\lambda_t + 2\mu_t)e - \gamma_t \theta, \quad (13)$$

where

$$e = \frac{\partial u}{\partial x}, \quad (14)$$

and the equations of motion will be reduced to

$$(\lambda_t + 2\mu_t) \frac{\partial^2 u}{\partial x^2} - \gamma_t \frac{\partial \theta}{\partial x} = \rho_t \frac{\partial^2 u}{\partial t^2}. \quad (15)$$

3. Mathematical approach to the issue

Seeing the refined Lord–Shulman system, Equations (15), (12), and (13) will be stated in the system of fractional order as

$$\frac{\partial^2 u}{\partial x^2} - c_1 \frac{\partial \theta}{\partial x} = \frac{1}{c_p^2} \frac{\partial^2 u}{\partial t^2}, \quad (16)$$

$$C_T^2 \frac{\partial^2 \theta}{\partial x^2} = \left(1 + \sum_{n=1}^N \frac{\tau^{n+\nu}}{(n+\nu)!} \frac{\partial^{n+\nu}}{\partial t^{n+\nu}}\right) \left[\left(w_b \rho_c + \frac{\partial}{\partial t}\right) \theta + \eta \frac{\partial^2 u}{\partial t \partial x}\right] - Q_0, \quad (17)$$

$$\frac{\sigma}{\lambda_t + 2\mu_t} = \frac{\partial u}{\partial x} - c_1 \theta, \quad (18)$$

where

$$c_1 = \frac{\gamma_t}{\lambda_t + 2\mu_t}, \quad C_P^2 = \frac{\lambda_t + 2\mu_t}{\rho_t}, \quad C_T^2 = \frac{k_t}{\rho_t c_t}, \quad \rho_c = \frac{\rho_b c_b}{\rho_t c_t}, \quad \eta = \frac{\gamma_t T_b}{\rho_t c_t}, \quad Q_0 = \frac{Q_m}{\rho_t c_t}. \quad (19)$$

With the initial conditions

$$u(x, t)|_{t=0} = \frac{\partial^{n+\nu} u(x, t)}{\partial t^{n+\nu}} \Big|_{t=0} = 0, \quad \theta(x, t)|_{t=0} = \frac{\partial^{n+\nu} \theta(x, t)}{\partial t^{n+\nu}} \Big|_{t=0} = 0, \quad n \geq 1. \quad (20)$$

It is presumed that the biological tissue is adhered to both the top and bottom surfaces. The upper surface of the

skin tissue experiences thermal loading, and the bottom surface, which has already reached the rated temperature, vanishes. In light of this, the boundary conditions are described as

$$\theta(0, t) = g(t), \quad \left. \frac{\partial \theta(x, t)}{\partial x} \right|_{x=L} = 0, \quad u(0, t) = 0, \quad u(L, t) = 0, \tag{21}$$

where, as illustrated in Figure 1, $g(t)$ represents the thermal load function on the upper face of the skin tissue. Consider the plane $x = 0$ of the tissue is labeled to ramp-type heat as

$$g(t) = \theta_0 \begin{cases} \frac{t}{t_0} & \text{if } 0 < t < t_0, \\ 1 & \text{if } t \geq t_0, \end{cases} \tag{22}$$

where $t_0 > 0$ is the ramp-type heating parameter and $\theta_0 > 0$ is the constant that symbolizes thermal loading.

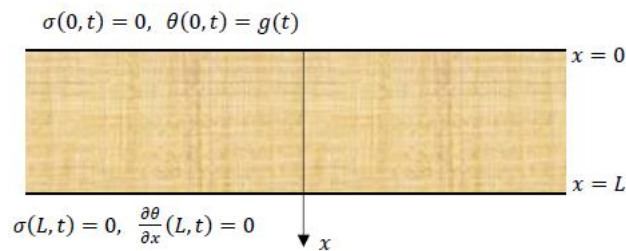


Fig. 1: The one-dimensional skin tissue with thermal and mechanical boundary conditions

4. Domain of the Laplace transform and its inversion

With the homogeneous initial conditions (20) and the Laplace transform on both sides of Eqs. (16) through (18), we obtain

$$\left(\frac{d^2}{dx^2} - c_2 \right) \bar{u} - c_1 \frac{d\bar{\theta}}{dx} = 0, \tag{23}$$

$$\left(\frac{d^2}{dx^2} - c_3 \right) \bar{\theta} = c_4 \frac{d\bar{u}}{dx} - \bar{Q}_1, \tag{24}$$

$$\frac{\bar{\sigma}}{\lambda_t + 2\mu_t} = \frac{d\bar{u}}{dx} - c_1 \bar{\theta}, \tag{25}$$

where

$$c_2 = \frac{s^2}{c_p^2}, \quad c_3 = \frac{w_b \rho_c + s}{c_T^2} \left(1 + \sum_{n=1}^N \frac{\tau^{n+\nu}}{(n+\nu)!} s^{n+\nu} \right), \tag{26}$$

$$c_4 = \frac{\eta s}{c_T^2} \left(1 + \sum_{n=1}^N \frac{\tau^{n+\nu}}{(n+\nu)!} s^{n+\nu} \right), \quad Q_1 = \frac{Q_0}{c_T^2}.$$

It is observed that the above bar character means its Laplace transform, s implies the Laplace parameter. Solving the system of Eqs. (23) and (24) in the Laplace field we get

$$\bar{\theta} = \sum_{i=1}^2 (A_i e^{\xi_i x} + B_i e^{-\xi_i x}) + \bar{Q}_2, \tag{27}$$

$$\bar{u} = \sum_{i=1}^3 \beta_i (A_i e^{\xi_i x} - B_i e^{-\xi_i x}), \tag{28}$$

where $\bar{Q}_2 = \bar{Q}_1/c_3$ and A_i and B_i are constant coefficients that differ on s . The inputs ξ_i and β_i are provided by

$$\xi_1, \xi_2 = \frac{1}{\sqrt{2}} \sqrt{c_1 c_4 + c_2 + c_3 \pm \xi_0}, \quad \xi_0 = \sqrt{(c_1 c_4 + c_2)^2 + c_3 [c_3 + 2(c_1 c_4 - c_2)]}, \quad (29)$$

$$\beta_i = \frac{\xi_i(\xi_i^2 - c_1 c_4 - c_3)}{c_2 c_4}. \quad (30)$$

Besides, the dilatation in Eq. (14) is assumed in the Laplace space by

$$\bar{e} = \sum_{i=1}^2 \beta_i \xi_i (A_i e^{\xi_i x} + B_i e^{-\xi_i x}). \quad (31)$$

Additionally, the axial stress corresponding to Eq. (25) develops into

$$\bar{\sigma} = \sum_{i=1}^2 \zeta_i (A_i e^{\xi_i x} + B_i e^{-\xi_i x}) - \bar{Q}_3, \quad (32)$$

where

$$\zeta_i = (\lambda_t + 2\mu_t)(\beta_i \xi_i - c_1), \quad \bar{Q}_3 = (\lambda_t + 2\mu_t)c_1 \bar{Q}_2. \quad (33)$$

The Laplace transform domain's boundary conditions (21) are provided by

$$\bar{\theta}(x, s) \Big|_{x=0} = \frac{\theta_0(1 - e^{-t_0 s})}{t_0 s^2} = \bar{G}_s, \quad (34)$$

$$\frac{\partial \bar{\theta}(x, s)}{\partial x} \Big|_{x=L} = 0, \quad \bar{u}(x, s) \Big|_{x=0, L} = 0. \quad (35)$$

The peculiar parameters A_i and B_i are stocked in the resolution of the substantial arrangement of direct conditions. Equations (27) and (28), by applying the aforementioned boundary conditions, get the following result:

$$\begin{bmatrix} 1 & 1 & 1 & 1 \\ \xi_1 e^{\xi_1 L} & -\xi_1 e^{-\xi_1 L} & \xi_2 e^{\xi_2 L} & -\xi_2 e^{-\xi_2 L} \\ \beta_1 & -\beta_1 & \beta_2 & -\beta_2 \\ \beta_1 e^{\xi_1 L} & -\beta_1 e^{-\xi_1 L} & \beta_2 e^{\xi_2 L} & -\beta_2 e^{-\xi_2 L} \end{bmatrix} \begin{Bmatrix} A_1 \\ B_1 \\ A_2 \\ B_2 \end{Bmatrix} = \begin{Bmatrix} \bar{G}_s - \bar{Q}_2 \\ 0 \\ 0 \\ 0 \end{Bmatrix}. \quad (36)$$

We solved the aforementioned system of linear equations to get the following parameters to finish the solutions in the Laplace transform domain:

$$A_1 = \frac{1}{\Delta} \beta_2 (\bar{Q}_2 - \bar{G}_s) (e^{(\xi_1 - \xi_2)L} - e^{(\xi_1 + \xi_2)L}), \quad (37)$$

$$B_1 = \frac{1}{\Delta} \beta_2 (\bar{Q}_2 - \bar{G}_s) (e^{(3\xi_1 - \xi_2)L} - e^{(3\xi_1 + \xi_2)L}), \quad (38)$$

$$A_2 = \frac{1}{\Delta} \beta_1 (\bar{G}_s - \bar{Q}_2) (e^{(\xi_1 - \xi_2)L} - e^{(3\xi_1 - \xi_2)L}), \quad (39)$$

$$B_2 = \frac{1}{\Delta} \beta_1 (\bar{G}_s - \bar{Q}_2) (e^{(\xi_1 + \xi_2)L} - e^{(3\xi_1 + \xi_2)L}), \quad (40)$$

in which

$$\Delta = (\beta_1 + \beta_2) (e^{(\xi_1 + \xi_2)L} - e^{(3\xi_1 - \xi_2)L}) + (\beta_1 - \beta_2) (e^{(\xi_1 - \xi_2)L} - e^{(3\xi_1 + \xi_2)L}). \quad (41)$$

It has now been entirely resolved for the transform domain. Given the difficulty of the formulations in Eqs. (27) and (28), achieving the inverse transform in the time domain analytically is not an easy task. So, the numerical inverse Laplace transform approach will be treated to ascertain the responses of temperature, displacement, and stress in the real-time domain. Numerical results are generated in the physical domain using the Riemann-sum approximation technique. Using the well-known equation, any function $\bar{f}(x, s)$ in the Laplace transform space is converted into a physical domain $f(x, t)$ in this approach [47]

$$f(x, t) = \frac{e^{qt}}{t} \left[\frac{1}{2} \operatorname{Re} \{ \bar{f}(x, \varrho) \} + \operatorname{Re} \left\{ \sum_{n=0}^N \left(\bar{f} \left(x, \varrho + \frac{i(n+\nu)\pi}{t} \right) (-1)^{(n+\nu)} \right) \right\} \right], \tag{42}$$

where Re is a function's real component, $i = \sqrt{-1}$, and $\varrho \approx 4.7/t$ [47].

5. Numerical outcomes

Here, we'll talk about the numerical findings related to temperature, displacement, and dilatation across the skin tissue. It will be discussed how fractional order can be applied to the traditional CTE theory and the simple and refined L–S generalized thermoelasticity theories. Table 1 shows the elastic constants of the blood and tissue.

Table 1: Elastic constants of skin biological tissue and blood.

Property	Value
Lame constant λ_t	$8.27 \times 10^8 \text{ kg}/(\text{m s}^2)$
Lame constant μ_t	$3.446 \times 10^7 \text{ kg}/(\text{m s}^2)$
Tissue density ρ_t	$1190 \text{ kg}/\text{m}^3$
Arterial blood temperature T_b	310 K
Tissue-specific heat c_t	3600 J/(K kg)
Tissue conductivity k_t	0.235 W/(m K)
Blood density ρ_b	$1060 \text{ kg}/\text{m}^3$
Blood specific heat c_b	3770 J/(K kg)
Linear thermal expansion α_t	$1 \times 10^{-4} \text{ (1/K)}$
Thickness of the skin tissue L	1 mm
Metabolic heat source Q_m	$368.1 \text{ W}/\text{m}^3$

Numerical results are appeared and presented in Figures 2-7. Figure 2 displays the distributions of temperature θ , displacement u , and dilatation e across the skin tissue using the thermoelasticity CTE, simple L–S, and refined L–S models with fractional effects eliminated ($\nu = 0$). A direct decrease in temperature along the x -axis is predicted by both the simple L–S and CTE theories. The revised L–S model has changed how the behavior appears. The temperature oscillates in the x direction due to the thickness of the skin tissue. The displacement achieves its maximum value for the CTE and simple L–S models at $x = 0.4$.

The simple L–S model produces the highest displacement at $u = 0.85$ at $x = 0.4$. Again, the new L–S line changes how displacement u looks. The displacement reaches its maximum value, $u = 0.6$, between $x = 0.3$ and $x = 0.7$. The dilatation reduces directly as x grows for the CTE and simple L–S curves. The revised L–S model alters how the behavior of dilatation e is seen. The dilatation e vibrates in the x direction. It's noteworthy to note that the dilatation e vanishes at $x = 0.4$ for all hypotheses.

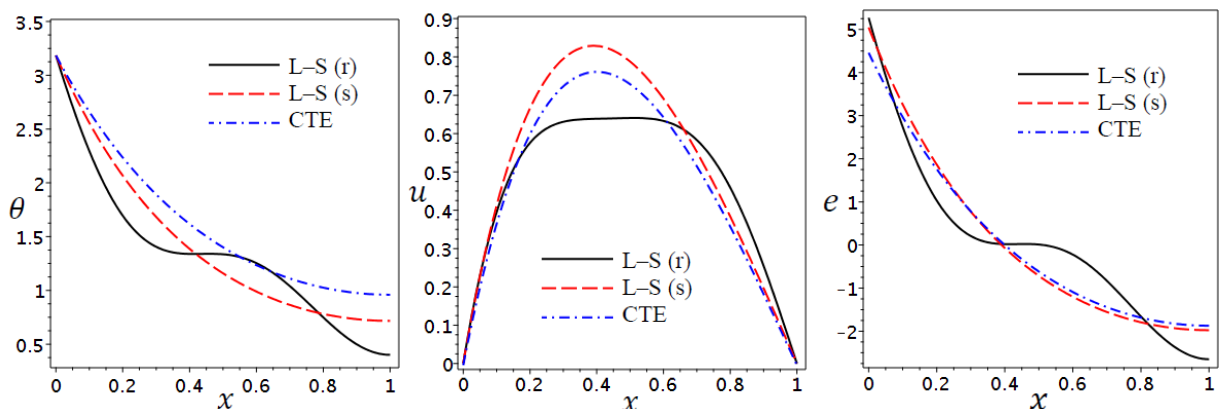


Fig. 2: Distributions of temperature θ , displacement u , and dilatation e during the skin tissue without the effect of fractions.

According to the thermoelasticity theories CTE, simple L–S, and refined L–S with fractional parameter $\nu = 0.8$, Figure 3 displays the distributions of temperature θ , displacement u , and dilatation e across the skin tissue. For the

CTE model, the temperature θ appears to be falling straight along the x direction. The temperature θ moves along the x axis for the simple L-S theory. When $x = 0.55$, θ begins to disappear. The refined L-S line states that the temperature θ declines gradually as x rises until $x = 0.5$, at which point it decreases directly along the x direction. The maximum displacement u for the CTE and simple L-S models occurs at $x = 0.4$, and the temperature θ is diminished at $x = 0.7$. The improved L-S model, where $u = 0.9$, has a maximum u value at $x = 0.6$. For all theories, the dilatation e falls off immediately. As x rises, the dilatation e reduces gradually until $x = 0.5$, at which point it decreases directly. For CTE and simple L-S theories, the dilatation e vanishes at $x = 0.4$, but it vanishes for the refined L-S theory at $x = 0.5$.

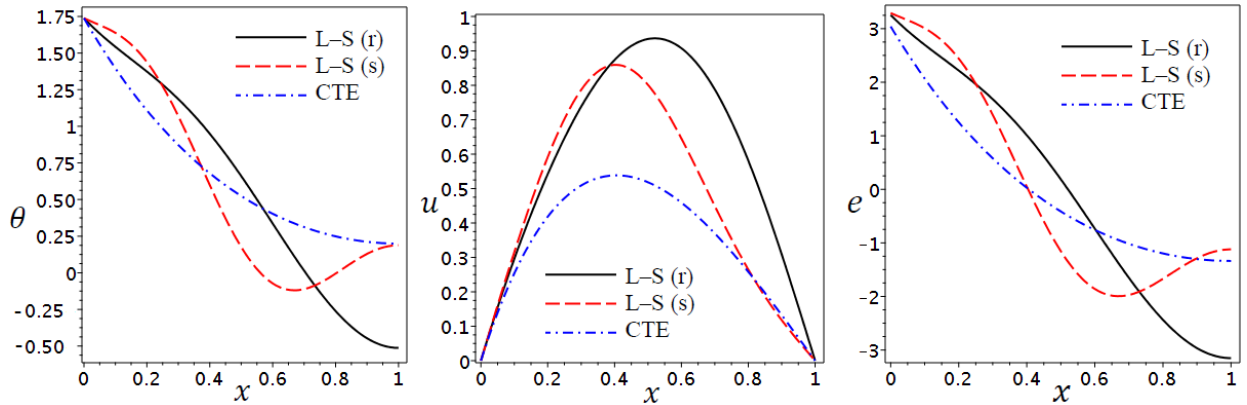


Fig. 3: Distributions of temperature θ , displacement u , and dilatation e during the skin tissue with fraction parameter $\nu = 0.8$.

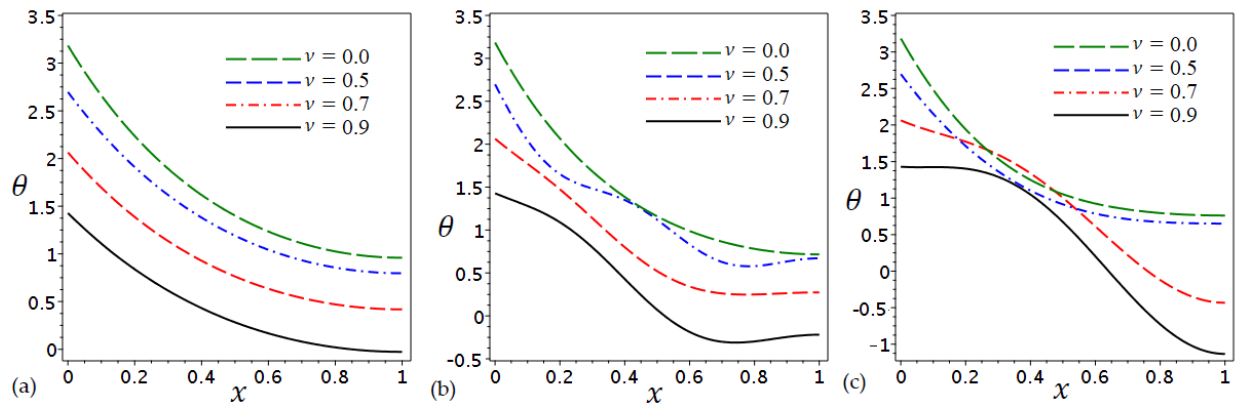


Fig 4: Distributions of temperature θ during the skin tissue according to (a) CTE, (b) Simple L-S and (c) Refined L-S with different fractional parameters.

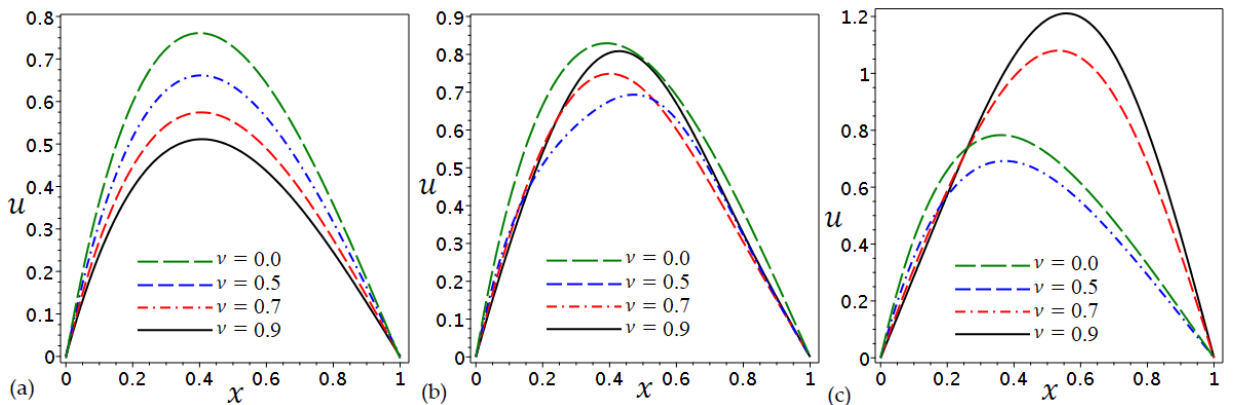


Fig 5: Distributions of displacement u during the skin tissue according to (a) CTE, (b) Simple L-S and (c) Refined L-S with different fractional parameters.

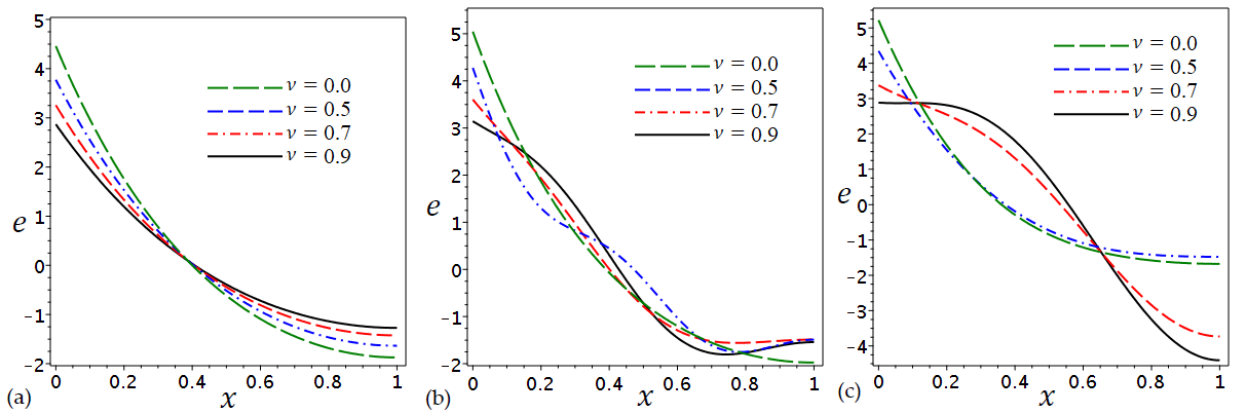


Fig 6: Distributions of dilatation e during the skin tissue according to (a) CTE, (b) Simple L–S and (c) Refined L–S with different fractional parameters.

As a second instance, the impacts of the fractional parameter ν on the temperature, displacement, and dilatation according to different theories are considered in Figures 4-6. Different values of the fractional parameter are applied in these figures. Once again, Figure 4 shows that the temperature θ , according to CTE, simple L–S and refined L–S through the skin tissue with different fractional parameters. The temperature θ in Figure 4(a), decreases directly for all values of ν and vanishes when $\nu = 0.9$ as $x = 1$. Furthermore, in Figure 4(b), the temperature θ , decreases directly for $\nu = 0$ and $\nu = 0.7$ and vibrates for $\nu = 0.5$ and $\nu = 0.9$ and it vanishes when $\nu = 0.9$ at $x = 0.5$. In Figure 4(c), the temperature θ decreases directly when $\nu = 0.5$ and $\nu = 0$. It vibrates when $\nu = 0.9$ and $\nu = 0.7$ and it vanishes when $\nu = 0.9$ at $x = 0.6$ and as $\nu = 0.7$, temperature θ vanishes at $x = 0.8$.

Figure 5 indicates that the displacement u , according to CTE, simple L–S and refined L–S theories through the skin tissue with different fractional parameters. Figure 5(a) shows that the displacement u has maximum values when $x = 0.4$ for all values of ν . The maximum value of the displacement u is $u = 0.7$ when $\nu = 0$, whereas the displacement u , in Figure 5(b) has maximum values when $x = 0.4$ for $\nu = 0.9$, $\nu = 0.7$, and $\nu = 0$ and has the maximum value at $x = 0.5$ when $\nu = 0.5$. The maximum value of the displacement u is $u = 0.8$ when $\nu = 0$. Figure 5(c) shows that the displacement u has maximum values when $x = 0.6$ for $\nu = 0.9$ and $\nu = 0.7$ and has maximum values at $x = 0.3$ for $\nu = 0.5$ and $\nu = 0$. The maximum value of the displacement u is $u = 1.20$ when $\nu = 0.9$.

Figure 6 indicates that the dilatation e according to CTE, simple L–S, and refined L–S theories through the skin tissue with different fractional parameters. In Figure 6(a), the dilatation e directly decreases during the skin tissue and vanishes when $x = 0.4$ for all values of ν . The dilatation e in Figure 5(b) directly decreases during the skin tissue for $\nu = 0$ and $\nu = 0.7$ and vibrates for $\nu = 0.5$ and $\nu = 0.9$. Once again, the dilatation e vanishes when $x = 0.5$ for $\nu = 0.5$ and vanishes at $x = 0.45$ for other values of ν . In Figure 5(c), dilatation e directly decreases during the skin tissue for $\nu = 0.5$ and $\nu = 0$ and vanishes as $x = 0.35$. The dilatation e vibrates for $\nu = 0.9$ and $\nu = 0.7$ and vanishes at $x = 0.6$.

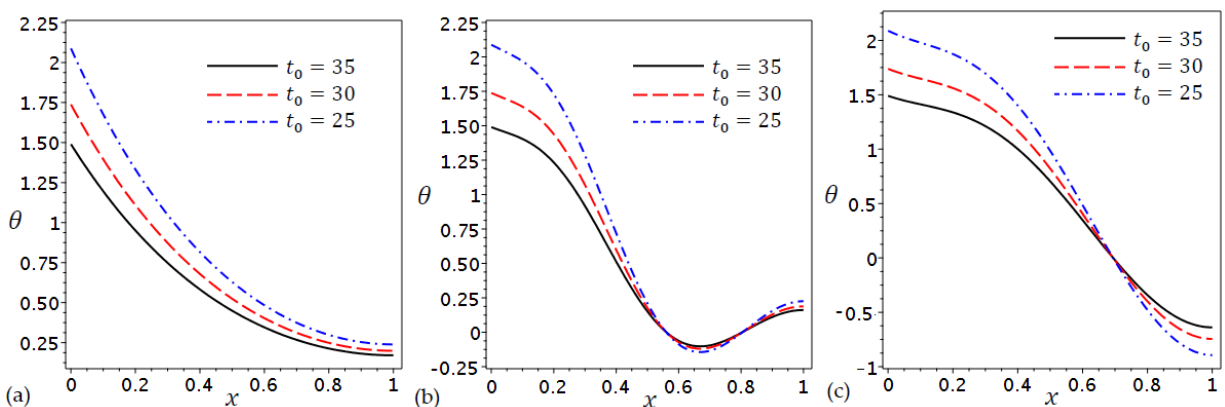


Fig 7: Distributions of temperature θ during the skin tissue according to (a) CTE, (b) Simple L–S and (c) Refined L–S with $\nu = 0.8$. and different values of ramp-type heat t_0 .

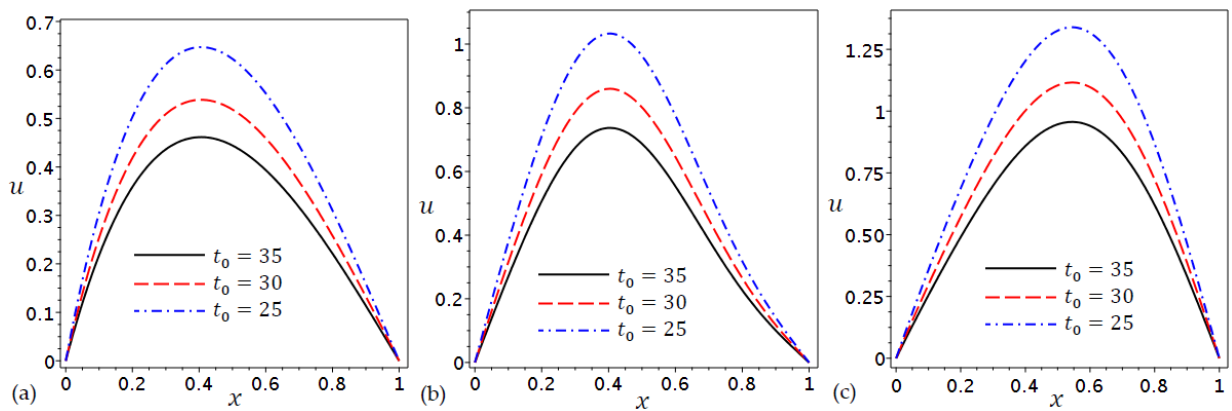


Fig 8: Distributions of displacement u during the skin tissue according to (a) CTE, (b) Simple L-S and (c) Refined L-S with $\nu = 0.8$. and different values of ramp-type heat t_0 .

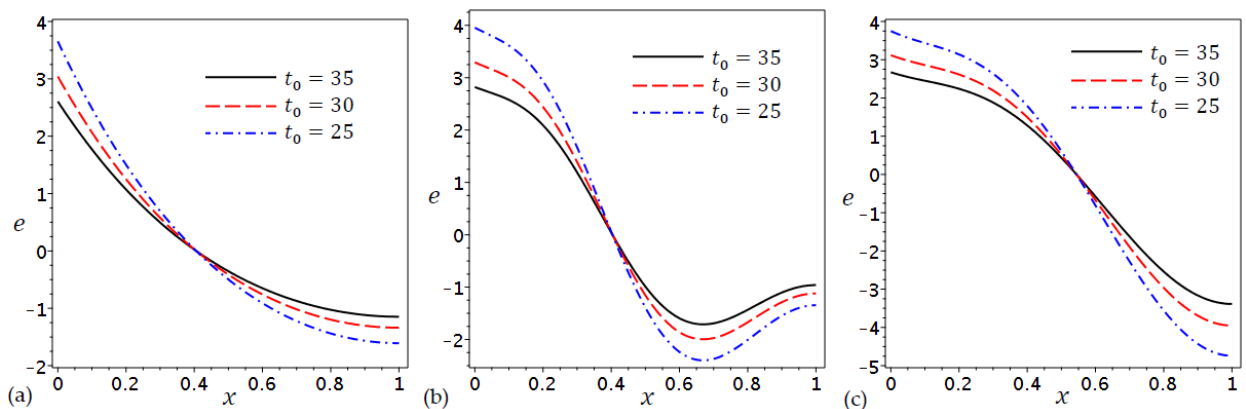


Fig 9: Distributions of dilatation e during the skin tissue according to (a) CTE, (b) Simple L-S and (c) Refined L-S with $\nu = 0.8$. and different values of ramp-type heat t_0 .

Figures 7-9, show that the effect of ramp-type heat t_0 on the behavior of temperature, displacement, and dilatation corresponding to distinct theories. In Figure 7 the difference between thermoelastic theories appeared on distributions of temperature θ during the skin tissue with different values of ramp-type heat t_0 . Figure 7(a) shows the impact of the ramp-type heat t_0 on temperature θ according to CTE, such that the higher value of ramp-type heat causes the lowest value of temperature θ . Furthermore, the impact of the ramp-type heat t_0 on temperature θ according to Simple (L-S) theory, shown in Figure 7(b). The temperature θ starts with different values and then gradually decreases until $x = 0.2$, then it decreases rapidly to vanish at $x = 5.5$, then the temperature θ for all three cases of the ramp-type heat t_0 oscillate at close values. The behavior of temperature θ in Figure 7(c) starts such that temperature θ decreases for all three cases of the ramp-type heat t_0 gradually until it reaches zero at $x = 5.5$, then the temperature θ which is affected by the smaller value of t_0 decreasing faster than the one which is affected by the largest value of t_0 .

As a second case, Figure 8 shows the difference between thermoelastic theories that appeared on distributions of displacement u during the skin tissue with different values of the ramp-type heat t_0 . It is clear that in Figure 8 the higher value of t_0 causes less displacement than the lower t_0 . Comparing the results of displacement u between in thermoelastic theories in Figure 8, it is clear that the displacement u according to CTE in Figure 8(a) has a maximum value at $x = 0.4$ for all values of t_0 such that $u = 0.455$ at $t_0 = 35$, $u = 0.545$ at $t_0 = 30$ and $u = 0.650$ at $t_0 = 25$. Furthermore, displacement u according to Simple (L-S) theory in Figure 8(b) has a maximum value at $x = 0.4$ for all values of t_0 such that $u = 0.754$ at $t_0 = 35$, $u = 0.850$ at $t_0 = 30$ and $u = 1.05$ at $t_0 = 25$. Finally, displacement u according to refined (L-S) theory in Figure 8(c) has a maximum value at $x = 0.55$ for all values of t_0 such that $u = 0.95$ at $t_0 = 35$, $u = 1.1$ at $t_0 = 30$ and $u = 1.35$ at $t_0 = 25$.

Figure 9 shows the difference between thermoelastic theories that appeared on distributions of dilatation e during the skin tissue with different values of the ramp-type heat t_0 . Figure 9(a) shows the distribution of dilatation e according to CTE. It shows the direct decrease of dilatation until $e = 0$ at $x = 0.4$ for all values of t_0 then dilatation is slowly decreasing for the large t_0 . In the same way, dilatation e directly decreases according to simple L-S until

$e = 0$ at $x = 0.4$, then it oscillates. Finally, dilatation e according to refined L–S is directly decreasing in Figure 9(c) until $x = 0.55$. then it slowly decreases for the higher value of t_0 .

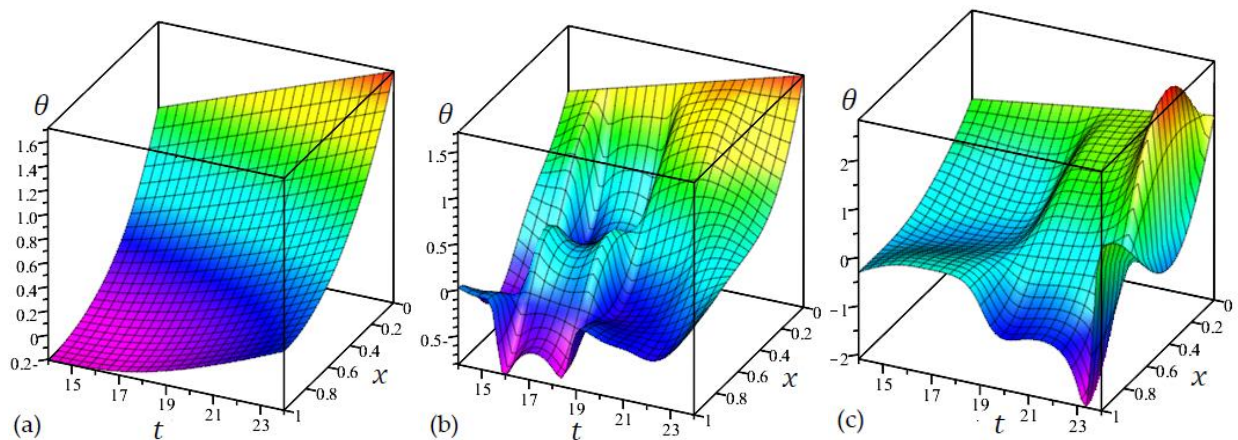


Fig 8: 3D Distributions of temperature θ during the skin tissue according to (a) CTE, (b) Simple (L–S) and (c) Refined (L–S) with fractional parameter $\nu = 0.8$.

The 3D plot is given to show the distributions of temperature $\theta(x, t)$, displacement $u(x, t)$ and dilatation $e(x, t)$ during the skin tissue corresponding to numerous theories with the effect of fractional parameter $\nu = 0.8$. Figure 10 shows that the fractional parameter $\nu = 0.8$ has a great effect on the distribution of the temperature $\theta(x, t)$ through the time t on the simple L–S and refined L–S models.

6. Conclusions

This study considers a newly evolved model of thermoelasticity with a new consideration of heat conduction with fractional-order theory with the Caputo fractional derivative of order ν . The present model is studied through one-dimensional small-thickness skin tissue under a ramp-type heat. The Solutions are achieved by using Laplace integral transform to analyze the data of the model. The numerical solutions for temperature θ , displacement u , and dilatation e are computed and clarified graphically. The outcome of the fractional order on the temperature θ , displacement u , and dilatation e according to different thermoelasticity theories CTE, simple L–S, and refined L–S appeared clearly in the figures. In the absence of the fractional operator's effect, it is noted that the CTE theory and the simple L–S behaviors due to temperature θ , displacement u , and dilatation e took the same shape. The influence of fractional derivatives is noted on the temperature θ . It is clear that the temperature values decrease, especially in simple L–S and refined L–S. In addition to that, displacement behavior is impressed, whereas it decreases according to CTE and increases according to Refined L–S. In all curves according to refined L–S, it is clear to note the difference in the shape of the curves of temperature θ , displacement u , and dilatation e .

Furthermore, comparing several values of ν on different theories of CTE, simple L–S and refined L–S, it is noted that the higher value of ν makes changes in the shape of temperature θ with lower values. That means the effect of fractional parameter on temperature causes weak conductivity and then it makes the change on displacement u , and dilatation e .

Based on the previous results, the solutions of the nondimensional temperature, displacement, stress, and strain distributions are significantly affected by the fractional-order parameter in the current model. The application of this study could be helpful in the uses of intensity move through organic tissues on a large scale, such as the use of lasers which rely on waves transferring heat in the treatment of skin diseases, cleaning burns from ruptured tissues, actinic keratosis, squamous cell carcinoma, and plastic surgery.

References

- [1] N. Fox, Generalised thermoelasticity, *International Journal of Engineering and Science*, Vol. 7, pp. 437-445, 1969.
- [2] A.M. Zenkour, T. Saeed and A.M. Aati, Refined Dual-Phase-Lag Theory for the 1D Behavior of Skin Tissue under Ramp-Type Heating, *Materials*, Vol. 16, pp. 2421, 2023.
- [3] M.A. Biot, Thermoelasticity and irreversible thermodynamics, *Journal of Applied Physics*, Vol. 27, pp. 240-253, 1956.

- [4] H.W. Lord and Y.A. Shulman, Generalized dynamical theory of thermoelasticity, *Journal of Mechanics and Physics of Solids*, Vol. 15, pp. 299-309, 1967.
- [5] A.E. Green and K.A. Lindsay, Thermoelasticity, *Journal of Elasticity*, Vol. 2, pp. 1-7, 1972.
- [6] D.S. Chandrasekharaiah, Hyperbolic thermoelasticity: a review of recent literature, *Applied Mechanics Reviews*, Vol. 51, pp. 705-729, 1998.
- [7] R.B. Hetnarski, and J. Ignaczak. Generalized thermoelasticity, *Journal of Thermal Stresses*, Vol. 22, pp. 451-476, 1999.
- [8] J. Ignaczak and O-S. Martin, Thermoelasticity with Finite Wave Speeds. OUP Oxford, 2009.
- [9] H.H. Sherief, Fundamental solution of the generalized thermoelastic problem for short times. *Journal of Thermal Stresses*, Vol. 9, pp. 151-164, 1986.
- [10] M.A. Ezzat and A.S. El-Karamany. The uniqueness and reciprocity theorems for generalized thermo-viscoelasticity with two relaxation times, *International Journal of Engineering Science*, Vol. 40, pp. 1275-1284, 2002.
- [11] S. Sharma, K. Sharma and R.R. Bhargava, Effect of viscosity on wave propagation in anisotropic thermoelastic with Green–Naghdi theory type-II and type-III, *Materials Physics and Mechanics*, Vol. 16, pp. 144-158, 2013.
- [12] M. I. Othman and E. M. Abd-Elaziz, Influence of gravity and microtemperatures on the thermoelastic porous medium under three theories, *International Journal of Numerical Methods for Heat & Fluid Flow*, Vol. 29, pp. 3242-3262, 2019.
- [13] K. Sharma and P. Kumar, Propagation of plane waves and fundamental solution in thermoviscoelastic medium with voids, *Journal of Thermal Stresses*, Vol. 36, pp. 94-111, 2013.
- [14] P. Lata, R. Kumar and N. Sharma. Plane waves in an anisotropic thermoelastic, *Steel and Composite Structures*, Vol. 22, pp. 567-587, 2016.
- [15] A.D. Hobiny and I.A. Abbas, Analytical solutions of the temperature increment in skin tissues caused by moving heating sources, *Steel and Composite Structures*, Vol. 40, pp. 511-516, 2021.
- [16] A.M. Zenkour and I.A. Abbas, A generalized thermoelasticity problem of an annular cylinder with temperature-dependent density and material properties. *International Journal of Mechanics and Sciences*, Vol. 84, pp. 54-60, 2014.
- [17] A.E. Green and P.M. Naghdi, A re-examination of the basic postulates of thermomechanics, *Royal Society*, Vol. 432, pp. 171-194, 1991.
- [18] A.E. Green, and P.M. Naghdi, On undamped heat waves in an elastic solid, *Journal of Thermal Stresses*, Vol. 15, pp. 253-264, 1992.
- [19] A.E. Green, and P.M. Naghdi, Thermoelasticity without energy dissipation, *Journal of Elasticity*, Vol. 31, pp. 189-208, 1993
- [20] D.S.A. Chandrasekharaiah, Uniqueness theorem in the theory of thermoelasticity without energy dissipation, *Journal of Thermal Stresses*, Vol. 19, pp. 267-272, 1996.
- [21] R. Kumar, A.K. Vashishth and S. Ghangas, Phase-lag effects in skin tissue during transient heating, *International Journal of Applied Mechanics and Engineering*, Vol. 24, pp. 603-623, 2019.
- [22] S.K. Sharma and D. Kumar, A study on non-linear DPL model for describing heat transfer in skin tissue during hyperthermia treatment, *Entropy*, Vol. 22, 481, 2020.
- [23] S. Chiriță and M. Ciarletta, Reciprocal and variational principles in linear thermoelasticity without energy dissipation, *Mechanics Research Communications*, Vol. 37, pp. 271-275, 2010.
- [24] J. Ghazanfarian, Z. Shomali and A. Abbassi, Macro-to nanoscale heat and mass transfer: the lagging behavior, *International Journal of Thermophysics*, Vol. 36, pp. 1416-1467, 2015.
- [25] M.I.A. Othman and I.A. Abbas, Generalized thermoelasticity of thermal-shock problem in a non-homogeneous isotropic hollow cylinder with energy dissipation, *International Journal of Thermophysics*, Vol. 33, pp. 913-923, 2012.
- [26] H.H. Sherief and W.E. Raslan, A 2D problem of thermoelasticity without energy dissipation for a sphere subjected to axisymmetric temperature distribution, *Journal of Thermal Stresses*, Vol. 40, pp. 1461-1470, 2017.
- [27] A.M. Zenkour, T. Saeed and K.M. Alnefaie, Refined Green–Lindsay model for the response of skin tissue under a ramp-type heating, *Mathematics*, Vol. 11, 1437, 2023.
- [28] R.L. Bagley and P.J. Torvik, On the fractional calculus model of viscoelastic behavior, *Journal of Rheology*, Vol. 30, pp. 133-155, 1999.
- [29] M.A. Ezzat and A.S. El-Karamany, Fractional-order theory of a perfect conducting thermoelastic medium, *Canadian Journal of Physics*, Vol. 89, pp. 311-318, 2011.

- [30] M.H. Hendy, M.M. Amin and M.A. Ezzat, Two-dimensional problem for thermoviscoelastic materials with fractional-order heat transfer, *Journal of Thermal Stresses*, Vol. 42, pp. 1298-1315, 2019.
- [31] I.A. Abbas, Eigenvalue approach to fractional-order generalized magneto-thermoelastic medium subjected to moving heat source, *Journal of Magnetism and Magnetic Materials*, Vol. 377, pp. 452-459, 2015.
- [32] N. Sharma, R. Kumar and P. Lata, Disturbance due to inclined load in transversely isotropic thermoelastic medium with two temperatures and without energy dissipation, *Materials Physics and Mechanics*, Vol. 22, pp. 107-117, 2015.
- [33] I.A. Abbas, Eigenvalue Approach for an unbounded medium with a spherical cavity based upon two-temperature generalized thermoelastic theory, *Journal of Mechanical Science and Technology*, Vol. 28, pp. 4193-4198, 2014.
- [34] M.A. Ezzat and M.Z. Abd-Elaal, Free convection effects on a viscoelastic boundary layer flow with one relaxation time through a porous medium, *Journal of the Franklin Institute*, Vol. 334, pp. 685-706, 1997.
- [35] H.H. Sherief, A.M.A. El-Sayed and A.M. Abd El-Latif, Fractional Order Theory of Thermoelasticity, *International Journal of Solids and Structures*, Vol. 47, pp. 269-275, 2010.
- [36] H.H. Sherief and W.E. Raslan, 2D Problem for a long cylinder in the fractional theory of thermoelasticity, *Journal of Solids and Structures*, Vol. 13, pp. 1596-1613, 2016.
- [37] M.H. Hendy, S.I. El-Attar and M.A. Ezzat, Two-temperature fractional Green–Naghdi of type iii in magneto-thermo-viscoelasticity theory subjected to a moving heat source, *Indian Journal of Physics*, Vol. 95, pp. 657-671, 2021.
- [38] P.J. Chen and M.E. Gurtin, On a theory of heat conduction involving two temperatures, *Zeitschrift Für Angewandte Mathematik Und Physik (ZAMP)*, Vol. 19, pp. 614-627, 1968.
- [39] M.A. Ezzat and E.S. Awad, Constitutive relations, uniqueness of solution, and thermal shock application in the linear theory of micropolar generalized thermoelasticity involving two temperatures, *Journal of Thermal Stresses*, Vol. 33, pp. 226-250, 2010.
- [40] I. Podlubny, *Fractional Differential Equations: An Introduction to Fractional Derivatives, Fractional Differential Equations, to Methods of Their Solution and Some of Their Applications*, Academic Press, 1998.
- [41] K. Diethelm, *The Analysis of Fractional Differential Equations: An Application-oriented Exposition using Differential Operators of Caputo Type*, Springer, 2010.
- [42] I.A. Abbas and A.M. Zenkour, Semi-analytical and numerical solution of fractional-order generalized thermoelastic in a semi-infinite medium, *Journal of Computational and Theoretical Nanoscience*, Vol. 11, pp. 1592-1596, 2014.
- [43] A.A. Kilbas, M. Rivero, L. Rodriguez-Germa and J.J. Trujillo, Caputo linear fractional differential equations. IFAC Proceedings, Vol. 39, pp. 52-57, 2006.
- [44] M. A. Ezzat, A. S. El-Karamany, A. A. El-Bary and M. A. Fayik, Fractional calculus in one-dimensional isotropic thermo-viscoelasticity, *Comptes Rendus Mecanique*, Vol. 341, pp. 553-566, 2013.
- [45] Q. Zhang, Y. Sunan and J. Yang, Bio-heat response of skin tissue based on three-phase-lag model, *Scientific Reports*, Vol. 10, pp. 16421, 2020.
- [46] M. Sobhy and A.M. Zenkour, Refined Lord–Shulman theory for 1D response of skin tissue under ramp-type heat, *Materials*, Vol. 15, pp. 6292, 2022.
- [47] G. Honig and U. Hirdes, A method for the numerical inversion of the Laplace transform, *Journal of Computational and Applied Mathematics*, Vol. 10, pp. 113-132, 1984.